Subthreshold production of J/ψ mesons from the deuteron with the proposed Solenoidal Large Intensity Device

Tianbo Liu [1,2] Zhiwen Zhao [3,4] Mengchu Cai [5,6] Duane Byer,[3,4] and Haiyan Gao [3,4]

[1]*Key Laboratory of Particle Physics and Particle Irradiation (MOE), Institute of Frontier and Interdisciplinary Science,*
Shandong University, Qingdao, Shandong 266237, China

[2]*Southern Center for Nuclear-Science Theory (SCNT), Institute of Modern Physics, Chinese Academy of Sciences, Huizhou 516000, China*

[3]*Department of Physics, Duke University, Durham, North Carolina 27708, USA*

[4]*Triangle Universities Nuclear Laboratory, Durham, North Carolina 27708, USA*

[5]*School of Physics, Peking University, Beijing 100871, China*

[6]*CAS Key Laboratory of Theoretical Physics, Institute of Theoretical Physics, Chinese Academy of Sciences, Beijing 100190, China*

The electro- and photoproduction of the J/ψ meson near the threshold from the proton are relevant to the search of hidden charm pentaquark candidates reported by the LHCb collaboration, and the study of the contribution of the quantum chromodynamics (QCD) trace anomaly to the proton mass. It is also expected to be sensitive to the QCD van der Waals interaction, that is mediated by multigluon exchanges and expected to dominate the interaction between two hadrons with no common valence quarks. Subthreshold production of J/ψ from a nuclear target is expected to enhance such attractive interaction, and also allows for a direct probe of short range correlations inside a nucleus. With the high luminosity capability of the 12-GeV CEBAF facility at Jefferson Laboratory, high-precision data on J/ψ meson production from the proton are becoming available, providing also a reference for subthreshold J/ψ production from the deuteron. Data from the deuteron will establish the baseline for subthreshold J/ψ production from other nuclear targets. In this paper, we present our findings from a feasibility study of subthreshold J/ψ production from the deuteron using the proposed Solenoidal Large Intensity Device (SoLID), and discuss the potential physics impact of such data.

I. INTRODUCTION

The J/ψ meson has been a fascinating particle to physicists since its original discovery in the 1970s [1,2]. Its discovery—the discovery of the charm quark—played an important role in the establishment of the quark model as a credible description of nature. In recent years, the J/ψ meson has also played an important role in the search of multiquark states [3,4], one of the active frontiers since the establishment of the quark model [5,6]. Hadrons, as color singlet states, are composite particles made of quarks and gluons held together by strong interactions. Ordinary mesons are described as quark-antiquark states and ordinary baryons are described as three-quark states. Exotic mesons, such as glueballs, tetraquarks, and hybrid mesons, have quantum numbers that are impossible for a quark-antiquark configuration. Similarly, exotic baryons have constituents other than the three-quark configuration. The pentaquark is a type of exotic baryon whose minimum-quark content is five-quark. The quantum chromodynamics (QCD) is known as the fundamental theory of strong interactions in the framework of the Yang-Mills gauge theory with quarks and gluons as degrees of freedom. It allows the existence of multiquark states; however, due to the nonperturbative nature of QCD at low energy scales, first principle calculations of hadronic states and properties remain challenging. Hence experimental investigation of multiquark states is an important

approach to understand the dynamics of the strong interaction at the hadronic scale.

In 2015, the LHCb collaboration discovered two hidden charm pentaquark candidates, named as $P_c(4380)$ and $P_c(4450)$, in the channel $\Lambda_b \to J/\psi K^- p$ [7], which contains narrow peaks in the $J/\psi p$ invariant mass distribution. In 2019, LHCb followed up with an order of magnitude more data. They discovered another narrow pentaquark candidate $P_c(4312)^+$ and confirmed that $P_c(4450)^+$ consists of two narrow overlapping peaks, $P_c(4440)^+$ and $P_c(4457)^+$ [8]. In light of these developments, the production of J/ψ mesons near the threshold from protons with high precision has become ever more important and compelling. The 12-GeV CEABF at Jefferson Laboratory (JLab) provides excellent opportunities to study the production of J/ψ mesons near the threshold as demonstrated by the GlueX experiment in JLab Hall D first in 2019 [9] and again in 2023 [10] with more statistics. The GlueX collaboration reported on the measurement of the $\gamma p \to J/\psi p$ cross section for photon energies from 11.8 GeV down to the threshold energy of 8.2 GeV using a tagged photon beam. The results show that the total cross section falls toward the threshold less steeply than expected from two-gluon exchange models [11]. While the LHCb pentaquark candidates P_c^+ in principle could be produced in the s channel of this reaction, the GlueX results provide no evidence for these states. JLab experiment E12-16-007 [12] took data in

Hall C in spring 2019 on photoproduction of J/ψ on the proton from the threshold of 8.2 GeV to energies above the threshold for the production of the $P_c(4450)$ state. The results [13] have no signal on the $P_c(4450)$ state, but the proton gluonic gravitational form factors are extracted.

Another major physics motivation for precise information on the near threshold photoproduction cross section of the J/ψ meson from the proton is due to its connection to the QCD trace anomaly, which is predicted to contribute significantly to the mass of the proton. The proton, as the bound state of strong interaction, is fundamentally described in terms of quarks and gluons degrees of freedom in QCD. Thus, a decomposition of the proton mass can be investigated from the QCD energy-momentum tensor, which can be uniquely separated into a traceless part and a trace part following the procedure in Refs. [14,15]. According to the separation of the energy-momentum tensor, one can partition the proton Hamiltonian in terms of the quark energy, gluon energy, quark mass, and the trace anomaly contributions. The parameter that determines the trace anomaly contribution to the proton mass, which also contributes to the quark mass and quark energy pieces can be extracted via the purely real amplitude of the interaction between heavy quarkonium and light hadron at low energy [16,17]. The heavy quarkonium, such as J/ψ, is a strongly bound state of two heavy quarks with both the constituents' mass and the binding energy much larger than $\Lambda_{\text{QCD}} \approx 340$ MeV [18], the typical nonperturbative QCD scale. Thus, it can be utilized as a microscopic probe of the structure of light hadrons, such as the proton. The quarkonium-nucleon scattering $J/\psi N \rightarrow J/\psi N$ is related to the differential cross section of forward photoproduction $\gamma N \rightarrow J/\psi N$ process through the conventional vector meson dominance (VMD) approach [17].

In the last two decades or so, there has been a renewed interest in the QCD van der Waals interaction—mediated by multigluon exchanges—which is expected to dominate the interaction between two hadrons when they have no common valence quarks. Such an attractive interaction in the case of the $J/\psi - N$ has been confirmed by both the effective field theory method [19–22] and lattice QCD [23]. This van der Waals attractive interaction also leads to the prediction of a bound state between a J/ψ and a light nucleus [24]. Lattice QCD simulations [25] have been performed for both the charmonium and the strangeonium cases showing that the interaction between the charmonium/strangeonium and the nucleon/nucleus could be strong enough to form a bound state. The study of bound J/ψ nuclear states [26] from photoproduction off nuclear targets requires precise measurements of J/ψ photoproduction from the proton and the deuteron targets near the threshold. Subthreshold production of ϕ or J/ψ mesons from a nuclear target is expected to enhance such attractive interactions. The $\phi - N$ bound state was explored by a number of authors [27–30]. Gao, Lee, and Marinov [27] were the first to propose and showed that the subthreshold quasifree ϕ meson production inside a nuclear medium would enhance the probability for the formation of the $\phi - N$ bound state. Experimental demonstration of subthreshold production of ϕ and J/ψ mesons will be an important step towards searching and/or discovering aforementioned exotic QCD bound states.

Previously, "subthreshold" production of ϕ mesons from a deuterium target has been demonstrated by CLAS6 [31], in which the physical threshold of the ϕ meson photoproduction from the proton was determined by the detection acceptance of the decay kaon pair. A quasifree model is able to describe the differential cross section well [31], though the data have rather large statistical uncertainties. Subthreshold production of J/ψ meson was also attempted previously in Hall C at the 6-GeV CEBAF [32]. While no event was seen for such production, this null finding is not surprising as subthreshold cross sections are small, and 5.7 GeV used for the experiment is too far from the threshold of 8.2 GeV.

Recently Hatta *et al.* [33] proposed subthreshold photoproduction of J/ψ from nuclear targets as an independent test of the universality of the nucleon-nucleon short-range correlation in nuclear scattering processes, and the deuteron is presented as the reference nucleus for such a test. Wu and Lee [34] studied quasifree production of J/ψ from the nucleon inside the deuteron near the threshold, and found at forward proton scattering angles and low J/ψ momenta in the center-of-momentum (c.m.) frame of the $J/\psi - N$ subsystem, the differential cross section is dominated by the $J/\psi - N$ rescattering. Therefore, carefully designed experiments using a deuterium target will allow for the extraction of the $J/\psi - N$ potential. Both sub- and near-threshold production of J/ψ is advantageous in this case to access low J/ψ momentum, therefore the rescattering region.

From the experimental side, JLab Hall D has obtained preliminary results on J/ψ production on D, ^{4}He, C targets that show promising signs of subthreshold production. JLab CLAS12 also collected data on J/ψ production from deuterium and other nuclear targets, and analyses are underway. While the results from both Hall D and CLAS12 will be of limited statistics, they allow for a first look of the physics we discussed above. In this paper, we present a study of subthreshold real and quasireal photoproduction of J/ψ meson from the deuteron using the proposed Solenoidal Large Intensity Device (SoLID) in Hall A at JLab. Compared to JLab GlueX and CLAS12, SoLID can handle at least 2 orders of magnitude higher luminosity and has large acceptance and good resolution for detecting multiple final state particles. While our focus is on the subthreshold production, we also present results near the threshold—the comparison of the production mechanism of J/ψ from the deuteron between subthreshold and above the threshold may uncover interesting short-range physics such as the nucleon-nucleon short-range correlation, non-nucleonic configuration such as hidden color states [35]. Furthermore, data on subthreshold production of J/ψ from the deuteron compared to those of the ϕ meson [31] can uncover interesting QCD dynamics that might be reflected in the difference between charmonium and strangeonium production below the threshold on the proton. The rest of the paper is organized as follows. In Sec. II, we present an description of the SoLID and the experimental method for the subthreshold and near threshold J/ψ production from a deuterium target. In Sec. III, we present our results from the simulations including the experimental apparatus, and the model used in our study on $\gamma d \rightarrow J/\psi\, p(n)$ reaction. Finally in Sec. IV, we will conclude and provide future outlook.
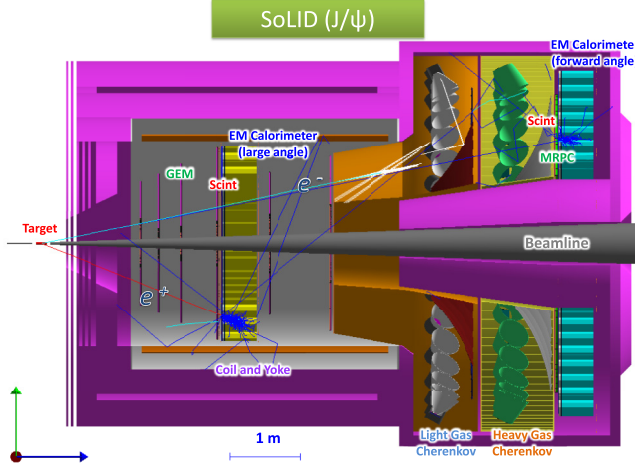
FIG. 1. The SoLID J/ψ experimental layout.

II. EXPERIMENTAL SETUP

The SoLID is a major new device combining large acceptance and high luminosity proposed for Hall A in the JLab 12-GeV era. The approved SoLID programs [36] consist of an experiment on parity-violating deep inelastic scattering [37] to provide an unique test of the standard model and search for new physics, experiments on semi-inclusive deep inelastic scattering to perform tomography of the nucleon in three-dimensional momentum space [38], and high precision measurements of cross sections from J/ψ electroproduction and photoproduction near the production threshold from the proton [39].

The J/ψ sub- and near-threshold production cross sections from the deuterium can be measured using the same experimental setup as that for the approved experiment [39] with a liquid deuterium target instead of a liquid hydrogen target. The layout of the SoLID J/ψ setup is shown in Fig. 1. With custom designed high rate and high radiation tolerant detectors, the SoLID J/ψ setup can carry out experiments using high intensity electron beams incident on a cryogenic target in an open geometry with a full azimuthal angular coverage. There are two groups of subdetectors. The forward angle detector group covers a polar angular range from $8°$ to $16°$ and consists of several planes of gas electron multipliers (GEM) for tracking, a light gas Cherenkov (LGC) for e/π separation, a heavy gas Cherenkov (HGC) for π/K separation, a multigap resistive plate chamber (MRPC) for time of flight, a scintillator pad (SPD) for photon rejection, and a forward-angle electromagnetic calorimeter (FAEC). The large-angle detector group covers a polar angular range from $18°$ to $28°$ and consists of several planes of GEM for tracking, an SPD and a large-angle electromagnetic calorimeter (LAEC). Electrons, positrons, and protons will be detected and identified by measuring their momenta, time of flight, photons produced in the threshold Cherenkov detectors, and energy losses in the calorimeters. A single particle geometrical acceptance is shown in Fig. 2 with the target center located at 315 cm upstream from the solenoid coil center. Limited by time-of-flight resolutions, the proton identification is good
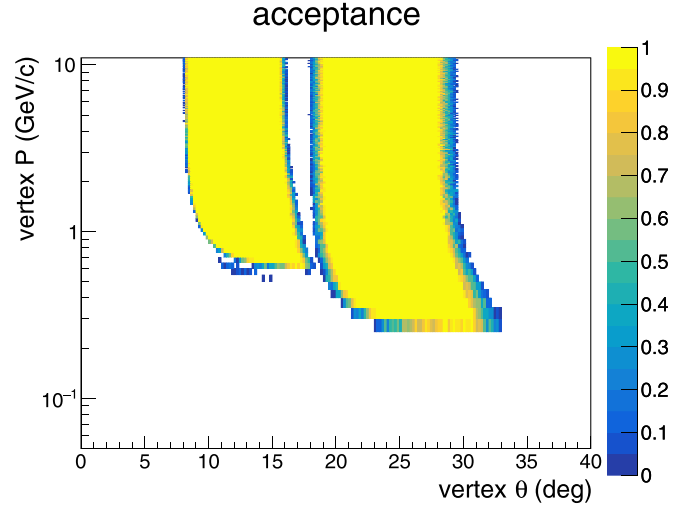
FIG. 2. The geometrical acceptance of a single particle in SoLID J/ψ setup at the forward angle (left) and large angle (right). The momentum and polar angle are from the particle vertex when it is produced at the target.

up to a momentum value of 4.5 GeV in the forward angular region and up to 2 GeV in the large angular region. While SoLID baseline detectors mentioned above do not provide a good capability for muon detection, a dedicated muon detector is being explored [40].

Because the subthreshold production is a rare process with small cross sections, we include both quasireal photoproduction (low Q^2 electroproduction) and real photoproduction to maximize event counts. As the proton detection requires the momentum greater than 0.2 GeV and there is no neutron detection capability in SoLID, we do not consider the production of J/ψ from the neutron inside a deuteron in our study. We require a three-fold coincident detection in which the J/ψ decay pairs of electron and positron as well as recoil protons will be detected. The detection of the scattered electrons is not required even in the case of the low Q^2 electroproduction. Thus the reactions of interest are $e^- + "p" \rightarrow (e^{-'}) + J/\psi + p \rightarrow (e^{-'}) + e^+ + e^- + p$ and $\gamma + "p" \rightarrow J/\psi + p \rightarrow e^- + e^+ + p$, where J/ψ is reconstructed through its decay into a lepton pair (e^+e^-) with a branching ratio of 5.94% and "p" stands for the proton inside the deuteron. The muon channel of J/ψ decay can be added to the same study once a SoLID muon detector is developed further.

In our study, the trigger used is the three-fold coincidence of the decay lepton pair and the recoil proton. There will be some four-fold electroproduction coincident events including the scattered electrons in the obtained data set for us to study and such a topology shall provide the best signal to background ratio but low statistics. One may choose to include only two-fold coincident detection of the J/ψ decay lepton pair if the trigger design allows, but it is expected to have large backgrounds for such a topology.

In our study, we use beam currents up to 1.25 μA to ensure the luminosity to stay below 1.2×10^{37} nucleon cm^{-2} s^{-1}, which is the same as that of the E12-12-006 experiment [39]. The SoLID collaboration is actively working on improving

the J/ψ setup's capability to handle even higher luminosity. If this effort is successful, one can increase the beam current for this experiment accordingly to achieve more statistics.

III. SIMULATION

To demonstrate the experimental feasibility of the sub-threshold and near-threshold J/ψ production from a deuterium target, we perform a Monte Carlo simulation using the proposed SoLID detector at JLab. In this section, we will briefly introduce the theoretical model of the photoproduction of J/ψ from the nucleon, and then describe the simulation procedure of the photoproduction and the electroproduction of J/ψ from a deuterium target. The simulation results are presented in the end of this section.

A. J/ψ photoproduction model

Although there are many phenomenological models for the J/ψ photoproduction from the nucleon, very few models can simultaneously describe the data at low and high energies, especially when including the precise data from JLab [9]. In a recent review [41], the Pomeron-potential model [42], referred to as the "Pom-pot" model, was found the only one that can fit data from near threshold [9] up to high energy $W = 300$ GeV [43]. Hence we use the differential cross section calculated by the Pom-pot model in the simulation.

The Pom-pot model is an extension of the Pomeron-exchange model. As advanced by Donnachie and Landshoff [44–47], the vector meson photoproduction at high energies can be well described by the Pomeron-exchange mechanism [48] and the vector meson dominance (VMD) assumption [49–52]. In this model, referred to as the "Pom-DL" model, the photon is first converted to the vector meson and then scattered by Pomeron-exchange between quarks in the vector meson and the nucleon. Though the Pom-DL model can well fit the J/ψ photoproduction data up to $W = 300$ GeV, the calculated cross section at low W is significantly below the recent JLab data. In such near threshold region, the relative velocity between J/ψ and the nucleon is not large and higher order multigluon exchanges that are not included in the Pomeron-exchange mechanism cannot be neglected. To solve this problem, it was proposed in Ref. [42] to add an effective $J/\psi - N$ potential term phenomenologically interpreted as the multigluon exchange.

With the VMD assumption, one can calculate J/ψ photoproduction cross section following the Hamiltonian

$$H = H_0 + V(r) + \frac{eM_{J/\psi}^2}{f_{J/\psi}} \int d^4x A_\mu(x) \phi^\mu(x), \qquad (1)$$

where $f_{J/\psi} = 11.2$ is the VMD coupling, which is evaluated from the decay width of $J/\psi \to e^+e^-$. $A_\mu(x)$ and $\phi^\mu(x)$ are the field operators of the photon and the J/ψ, respectively, e is the electric charge of the positron, and $M_{J/\psi}$ is the mass of the J/ψ meson. $V(r)$ is the $J/\psi - N$ potential, which can be extracted from lattice QCD calculation [23]. As found in Ref. [42], the lattice QCD data can be fitted by a

Yukawa form potential

$$V(r) = V_0 \frac{e^{-ar}}{r}, \qquad (2)$$

where V_0 and a are free parameters. Two sets of parameters, $V_0 = -0.06(-0.11)$ and $a = 0.3(0.5)$ GeV, are provided in Ref. [42] corresponding to two different selected fit regions of the lattice data, but the final numerical results are almost indistinguishable. More detailed discussions on the fit of the potential and the dependence on the parametrization form can be found in Ref. [42].

A feature of the VMD model using the lattice QCD potential is that the total cross section decreases at high energy, i.e., large W, where the data are orders of magnitude above the model prediction. A possible solution to this problem is to extend the VMD model by including the Pomeron exchange, which dominates the cross section at high energies. Although the $J/\psi - N$ potential at short distances, $r < 0.4$ fm, is difficult to be quantified from the lattice QCD calculation [23], the long-distance region, which accounts for the nonperturbative interaction, can be well extracted. The effect of the less constrained short-distance region is discussed in Ref. [42]. To develop a model which contains both nonperturbative and perturbative mechanisms, one can formally add a perturbative potential term $V_{pQCD}(r)$ into the Hamiltonian. The photoproduction amplitude will then obtain a term from $V_{pQCD}(r)$ in addition to the amplitude in the original VMD model. Due to the absence of perturbative potential, one can further replace the amplitude from the $V_{pQCD}(r)$ term by the amplitude from the Pomeron-exchange model [26,53], which is developed based on the perturbative analysis of Donnachie and Landshoff [44].

By fitting the JLab data [9], it was also observed that a rescaling factor $F^{off} = 0.4(0.7)$ to the VMD coupling $1/f_{J/\psi}$ was necessary to describe the near-threshold region while the fit to high energy region is also improved. The introduction of such a correction factor can be interpreted as the scale dependence of the coupling and is consistent with the study of ρ photoproduction [46]. The real photon considered here has invariant mass square $q^2 = 0$, which is very different from the decay process $J/\psi \to \gamma \to e^+e^-$ with $q^2 = M_{J/\psi}^2 \approx 9$ GeV^2, conventionally used to determine the VMD coupling. Then the resulting Pom-pot model can describe data from near threshold up to $W = 300$ GeV [41].

In Fig. 3, we show the differential cross section of the photoproduction of J/ψ from the nucleon at several W values near the threshold. More comprehensive comparison between the model predictions and experimental data, as well as the comparison among different models, can be found in Ref. [41].

B. Simulation of J/ψ production from a deuterium target

In this subsection, we describe the approach to simulate the photoproduction and the electroproduction of J/ψ from a deuterium target, using the differential cross section of the photoproduction from the nucleon as a model input.

As a baseline estimation, we only consider the quasifree mechanism of the production from the deuteron, and
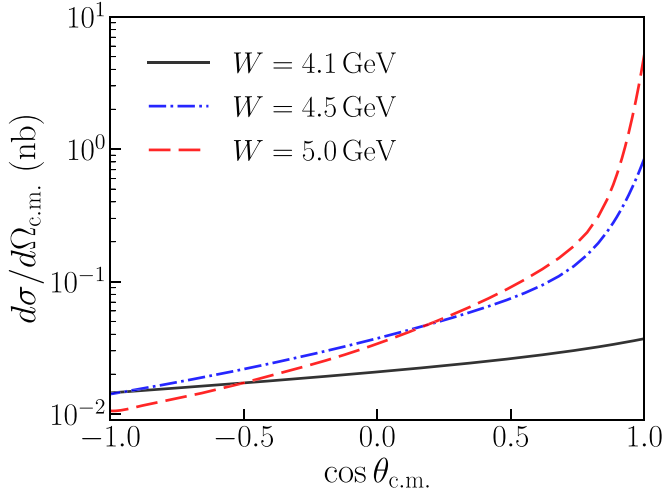
FIG. 3. The differential cross section of the photoproduction of J/ψ from the nucleon in the Pom-pot model. The angles $\Omega_{\text{c.m.}}$ and $\theta_{\text{c.m.}}$ are defined in the center-of-mass frame with the photon moving along the z direction.

final-state interaction effects are neglected. In the quasifree mechanism, subthreshold production is possible because of the Fermi motion of the nucleons in the deuteron nucleus. Here, we use a two-pole parametrization [54] of the deuteron wave function

$$\widetilde{\Psi}(\mathbf{p}) = \frac{1}{\sqrt{c}} \left[\frac{1}{\mathbf{p}^2 + a^2} - \frac{1}{\mathbf{p}^2 + b^2} \right], \tag{3}$$

where the parameter $a = 0.0456\,\text{GeV}$ is determined by the position of the nucleon pole, $b = 0.2719\,\text{GeV}$ is determined empirically from the average deuteron size, and c is a normalization factor [55]. The momentum distribution of the nucleon in the deuteron is then given by the square of the wave function, $|\widetilde{\Psi}(\mathbf{p})|^2$. As shown in Ref. [55], the two-pole parametrization provides an excellent approximation to the realistic wave function in a wide range of momentum. In comparison with the solution from the AV18 NN potential [56], the two-pole parametrization agrees well with the realistic momentum distribution up to $|\mathbf{p}| \approx 0.3\,\text{GeV}/c$, but underestimates the density at the high momentum region because of the absence of the D-wave component. Since this deviation will only result in possible underestimates of the signal rate for the subthreshold and near-threshold productions, it will not affect the conclusion of the feasibility study in this paper.

As the simplest nucleus, the deuteron only contains two nucleons, and thus the momenta of the two nucleons is always back to back with the same magnitude in the deuteron rest frame. In the impulse approximation, one of the bound nucleons is struck by the photon to produce the J/ψ as well as the recoil nucleon, while the spectator nucleon keeps its momentum as in the initial state. Then we can solve the energy of the struck nucleon

$$E_N = M_d - \sqrt{M_N^2 + \mathbf{p}^2}, \tag{4}$$

where M_d and M_N are the deuteron mass and the nucleon mass, respectively. In the simulation, we randomly sample the nucleon momentum according to the distribution given by the wave function (3) and then calculate its off-shell energy from Eq. (4). The J/ψ events are generated via the subprocess $\gamma + \text{"}p\text{"} \rightarrow J/\psi + p$ using the differential cross section from the Pom-pot model [42]. For the detection reason, we only consider the production from the proton inside the deuteron.

For the photoproduction, the target itself serves as the radiator. In the simulation, we generate photons according to an approximate distribution of the Bremsstrahlung spectrum [57],

$$\frac{dN_\gamma}{dE_\gamma} = \frac{d}{X_0} \frac{1}{E_\gamma} \left(\frac{4}{3} - \frac{4}{3} y + y^2 \right), \tag{5}$$

where E_γ is the photon energy, y is the energy ratio between the Bremsstrahlung photon and the electron beam, d is the radiator length, and X_0 is the radiation length of the target. The direction of the Bremsstrahlung photons is assumed along the beam direction. For liquid deuterium target, $X_0 = 769.1\,\text{cm}$. In this study, we use an $8.5\,\text{GeV}$ electron beam incident on a 15-cm long liquid deuterium target. Since the target is utilized as the radiator, the effective radiator length for the photoproduction is half of the target length, corresponding to $d/X_0 \approx 0.98\%$.

For the electroproduction, we consider the J/ψ production from the subprocess $\gamma^* + \text{"}p''\text{"} \rightarrow J/\psi + p$, where γ^* is the virtual photon. At the leading order of α, the electromagnetic fine structure constant, we can relate the electroproduction cross section to that of the photoproduction as shown in the formula below with details described in the Appendix,

$$\frac{E' d\sigma_{eN \rightarrow e'J/\psi N}}{d^3\mathbf{l}' d\Omega_{\text{c.m.}}} = \frac{\alpha}{2\pi^2(1-\epsilon)Q^2} \frac{\sqrt{(q \cdot p)^2 - q^2 p^2}}{\sqrt{(l \cdot p)^2 - l^2 p^2}}$$
$$\times \frac{d\sigma_{\gamma^* N \rightarrow J/\psi N}}{d\Omega_{\text{c.m.}}}, \tag{6}$$

where l, $l' = (E', \mathbf{l}')$, $q = l - l'$, and p are the four-momenta of the incoming electron, the scattered electron, the virtual photon, and the initial nucleon, respectively. $Q^2 = -q^2$ is the virtuality of the photon, and ϵ is the ratio between the timelike (also referred to as longitudinal) polarized and transverse polarized photons. This reaction is dominated by the low-Q^2 region, in which case it is referred to as quasireal photoproduction.

In this study, both the photoproduction and the electroproduction processes are simulated. For electroproduction, the event rate is low if we require that the scattered electrons are detected by the subdetectors of SoLID. Thus we choose to focus only on quasireal photoproduction where the scattered electrons travel near the incoming electron beam direction and escape the SoLID. In this case, events from real and quasireal photoproductions are indistinguishable. The photon fluxes from these two are roughly equal for a 8.5-GeV electron beam on a 15-cm long liquid deuterium target for a photon energy range from 7.2 GeV to 8.5 GeV.

The J/ψ mesons are reconstructed from the decay channel $J/\psi \rightarrow e^+ e^-$. The $e^+ e^-$ pair from the J/ψ decay is assumed
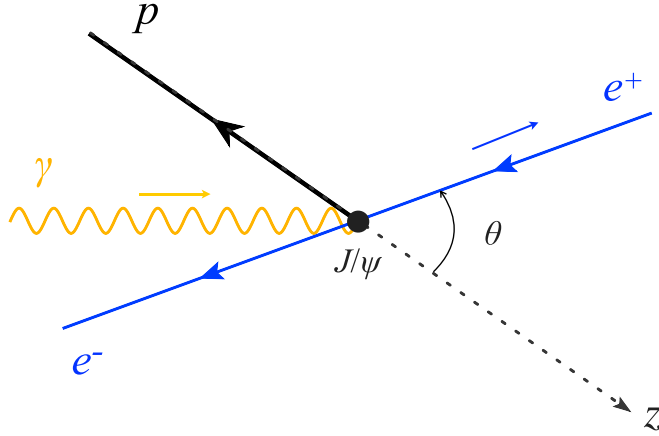
FIG. 4. The definition of the θ angle describing the decay angular distribution in the J/ψ rest frame in Eq. (7).

to follow the distribution [58]

$$f(\cos\theta) = \frac{3}{8\pi}[1 + \rho + (1 - 3\rho)\cos^2\theta], \qquad (7)$$

where

$$\rho = \frac{\epsilon R}{1 + \epsilon R} \qquad (8)$$

and [59,60]

$$R = \left(\frac{\lambda M_{J/\psi}^2 + Q^2}{\lambda M_{J/\psi}^2}\right)^n - 1. \qquad (9)$$

The parameters $\lambda = 2.164$ and $n = 2.131$ are determined phenomenologically [61]. As illustrated in Fig. 4, the angle θ of the positron is defined in the J/ψ rest frame with the recoil nucleon moving against the z direction.

For the study of subthreshold production of J/ψ mesons and the exploration of the $J/\psi - N$ interaction, we require a three-fold simultaneous detection of e^+, e^-, and p in the final state. The detection of the recoil proton is not only important for the reconstruction of the untagged photon energy, but also necessary for deriving the relative momentum of the $J/\psi - N$ system, which is essential to extract the $J/\psi - N$ interactions.

With only the detection of the momenta of J/ψ and the proton, one cannot determine the photon energy from the energy-momentum conservation for a general nuclear target. However, for the deuteron, as the simplest nucleus, the on-shell condition of the undetected nucleon in the final state provides an additional relation, which allow us to solve the photon energy as

$$E_\gamma = \frac{1}{2} \frac{(E_{J/\psi} + E_p - M_d)^2 - (\mathbf{p}_{J/\psi} + \mathbf{p}_p)^2 - M_n^2}{E_{J/\psi} + E_p - p_{J/\psi}^z - p_p^z - M_d}, \qquad (10)$$

where M_n is the mass of the undetected neutron, $E_{J/\psi}$ and E_p are the energies of the produced J/ψ and the proton, and $\mathbf{p}_{J/\psi}$ and $\mathbf{p}_p$ are their momenta with z components $p_{J/\psi}^z$ and p_p^z. This relation does not rely on the quasifree mechanism or the impulse approximation, and it is a unique advantage of the deuteron target.
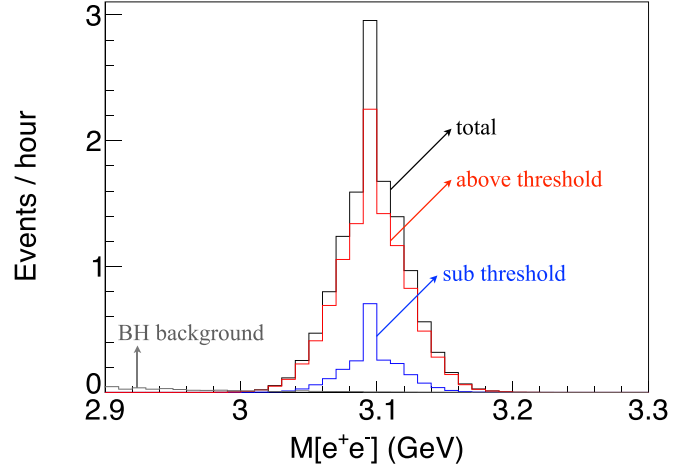

FIG. 5. J/ψ signal rate reconstructed from the e^+e^- decay channel. The lower blue curve is the production below the threshold, the middle red curve is the production above the threshold, the the upper black curve is the sum of subthreshold and above-threshold productions. The gray curve is the background from the Bethe-Heitler process.

As demonstrated in Ref. [34], when the relative momentum of the $J/\psi - N$ system is small, the reaction is more sensitive to the $J/\psi - N$ potential. To select the events in such region, we introduce the momentum of J/ψ in the $J/\psi - N$ c.m. frame, labeled as $\kappa_{J/\psi}$, which can be calculated from the momenta of the J/ψ and the proton as

$$\kappa_{J/\psi} = \frac{1}{2W}\sqrt{\left(W^2 - M_{J/\psi}^2 - M_p^2\right)^2 - 4M_{J/\psi}^2 M_p^2}. \qquad (11)$$

C. Simulation results

Following the procedure described above, we simulate the J/ψ production events using a 8.5 GeV electron beam with 1.25 µA current incident on a 15-cm liquid deuterium target, corresponding to the luminosity of 1.2×10^{37} nucleons cm^{-2} s^{-1}. This is the same as the luminosity of the approved SoLID J/ψ experiment using a liquid hydrogen target. This chosen 8.5 GeV energy is above the J/ψ but below the $J/\psi + \pi$ production threshold from the proton. The SoLID acceptance, as shown in Sec. II, is applied for final state particles. Since no neutron detection is designed in SoLID and the detection of protons requires the momentum greater than 0.2 GeV/c, we do not consider the J/ψ production from the neutron in the deuteron. To account for the detector resolution, the three-momenta of detected particles are randomly smeared with gaussian distributions according to the SoLID resolution described in Sec. II. For signal rate estimation, the results are scaled by a factor of 0.8 as the overall detection efficiency. All results in this subsection are the sum of real and quasireal photoproductions, since they are experimentally indistinguishable without the detection of the scattered electron.

In Fig. 5, we show the distribution of the invariant mass of the e^+e^- pair from the J/ψ decay. The width is dominated by the detector resolution since the intrinsic width of J/ψ

TABLE I. The event rates and the total counts in 47 days with the invariant mass of e^+e^- within the 120 MeV window around the J/ψ mass.

	events/hour	events in 47 days
subthreshold	2.1	2360
above threshold	10.3	11621
total	12.4	13981

is negligible. To suppress the background while keeping the signal events as many as possible, we choose a 120 MeV window, i.e., 3.04–3.16 GeV, around the J/ψ mass. The signal rates and the total counts in 47 days are listed in Table I. The well-known Bethe-Heitler (BH) process contains the same final state particles as J/ψ production. It could be the main background for the kinematics of study. We followed the recent BH calculation on deuteron [62] and carried out the same simulation. The resulting BH event rate is at sub-percent level comparing to the J/ψ as shown in Fig. 5.

Taking the unique advantage of the deuteron target, we can reconstruct the photon energy from Eq. (10) by a simultaneous detection of the recoil proton along with the two decay leptons from the J/ψ. The uncertainty of the determination of the photon energy depends on the detector resolution. In Fig. 6, we show the smearing of the reconstructed photon energy around the values recorded in the simulation. As labeled in the figure, the width of the smearing increases with the photon energy. The projection of the signal events in photon energy bins is shown in Fig. 7, where the statistical uncertainties are calculated from the square root of the number of events in the bins. The BH event rate is shown again at subpercent level comparing to the J/ψ for different photon energy.

FIG. 7. Projections in the photon energy in the simulation with electron beam energy $E = 8.5$ GeV. The horizontal width represents the binning and the vertical width represent the statistical uncertainty. The gray curve is the background from the Bethe-Heitler process.

The triple coincident detection of e^+, e^-, and p also allows us to reconstruct the J/ψ momentum in the $J/\psi - N$ c.m. frame via Eq. (11). We observe from the simulation that the events with higher recoil proton momentum favor lower values of $\kappa_{J/\psi}$. As demonstrated in Ref. [34], these events are more sensitive to the $J/\psi - N$ interaction. In Fig. 8, we show the projection in $\kappa_{J/\psi}$ bins. The projections by selecting events with the proton momentum below and above 1.0 GeV are also separately drawn. As shown in Fig. 9, the distributions of $\kappa_{J/\psi}$ in several photon energy intervals below the production threshold of 8.2 GeV, the expected statistics allows us to further bin the events in the photon energy, which will
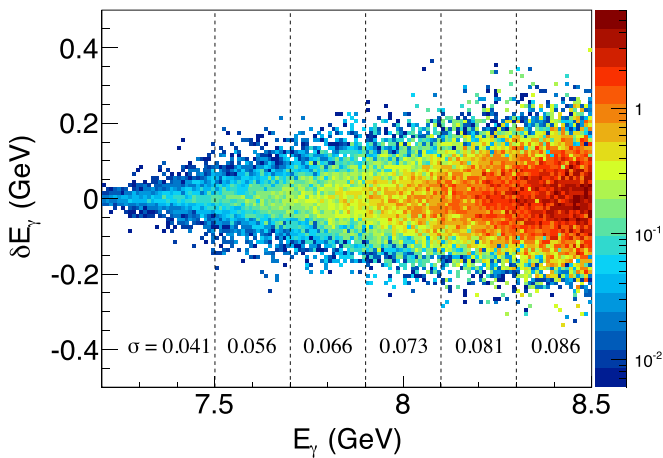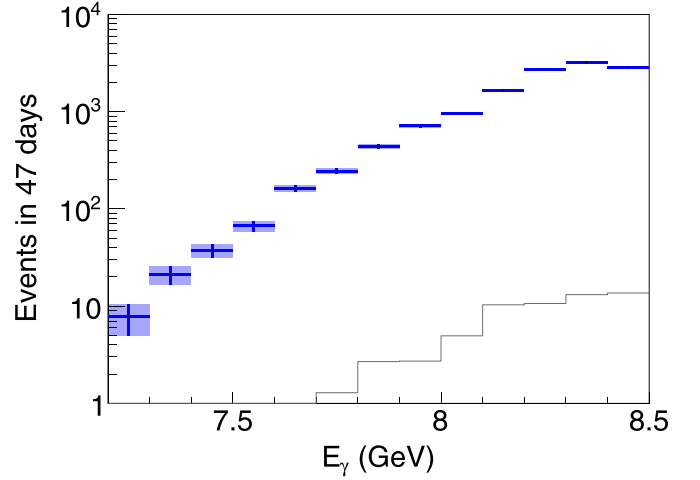

FIG. 6. The smearing of the reconstructed photon energy due to the detector resolution. E_γ is the photon energy recorded in the simulation with electron beam energy $E = 8.5$ GeV. δE_γ is the difference between the reconstructed photon energy and E_γ. The σ labels the standard deviation of δE_γ in each energy interval separated by vertical dashed lines. The color code represents the event rate distribution in the logarithmic scale.
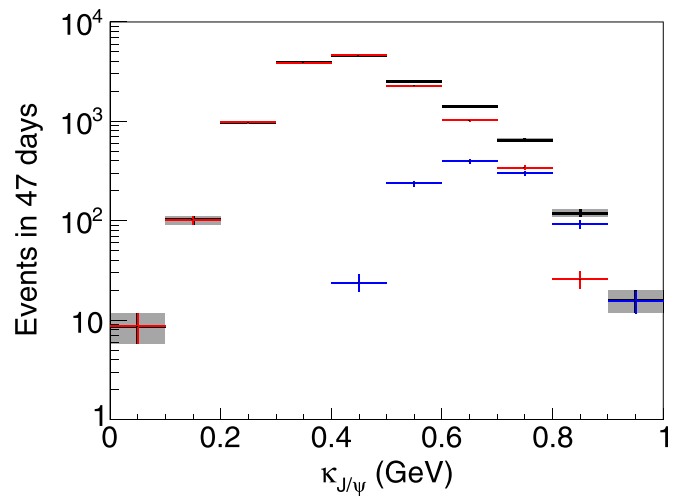

FIG. 8. Projections in the J/ψ momentum in the $J/\psi - N$ c.m. frame. The horizontal width represents the binning and the vertical width represents the statistical uncertainty. The blue points are the results with the proton momentum less than 1 GeV, the red points are the results with the proton momentum greater than 1 GeV, and the black points are the sum.
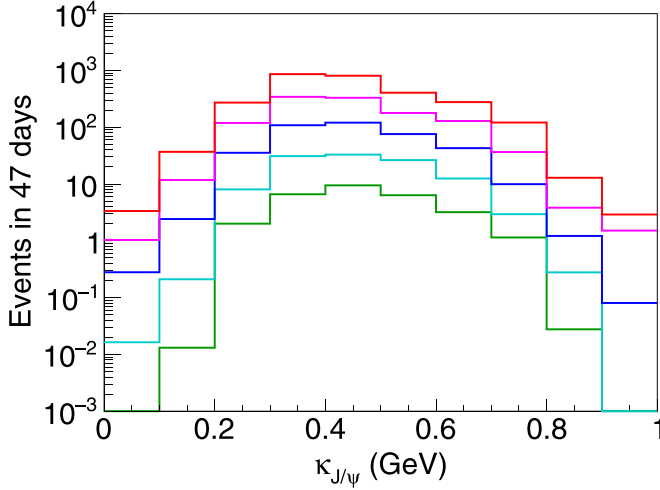
FIG. 9. Distributions of the J/ψ momentum in the $J/\psi - N$ c.m. frame from productions below the threshold. The curves from bottom to top correspond to the photon energy bins of [7.2, 7.4] GeV (green), [7.4, 7.6] GeV (cyan), [7.6, 7.8] GeV (blue), [7.8, 8.0] GeV (magenta), and [8.0, 8.2] GeV (red).

provide the opportunity of more detailed studies of the $J/\psi - N$ interaction.

IV. DISCUSSION AND CONCLUSIONS

With the unique capability of SoLID in combining high luminosity and large acceptance, our studies have shown that subthreshold production of J/ψ from the deuteron is experimentally feasible at JLab. The study on the deuteron also opens a new window for future studies of subthreshold production of J/ψ from other nuclei and the data on the deuteron will serve as reference. Such studies will be important to search for J/ψ-nuclear bound states and nuclear short-range correlations. Further, the projected quasifree J/ψ production data from the deuteron reported in this work, and future studies from other nuclei, near the production threshold of the proton can be compared with those from a free proton target to investigate any nuclear dependence in multi-gluon exchange. Such studies can also help answer the question of whether there might be medium modification of the matter radius of the proton.

J/ψ meson near- and subthreshold production from the deuteron is an important reaction to study nonperturbative QCD. Expanding from the proton, the production on the deuteron directly touches on many interesting QCD topics such as van der Waals interaction, multigluon exchange, bound states, short-range correlations, and gluonic gravitational form factors. While small cross section and multiple final state particle detection made this reaction a challenge to access in the past, the situation has changed since JLab entered the 12 GeV era. Our study demonstrated this exciting measurement is now feasible through the next generation high luminosity and large acceptance detector SoLID. The high quality data would open a new door to allow many advanced QCD studies with this unique reaction.

APPENDIX: RELATING ELECTROPRODUCTION AND PHOTOPRODUCTION CROSS SECTIONS

Here, we provide the derivation of Eq. (6), which relates the electroproduction cross section to the photoproduction cross section at the leading order of α.

The electroproduction cross section is

$$d\sigma_{eN \to e'J/\psi N} = \frac{|\mathcal{M}_{eN \to e'J/\psi N}|^2}{4\sqrt{(l \cdot p)^2 - l^2 p^2}} dPS, \quad (A1)$$

where $\mathcal{M}_{eN \to e'J/\psi N}$ is the invariant amplitude. The phase space is given by

$$dPS = (2\pi)^4 \delta^{(4)}(l + p - l' - p_{J/\psi} - p')$$
$$\times \frac{d^3 \mathbf{l}'}{2E'(2\pi^3)} \frac{d^3 \mathbf{p}'}{2E'_p(2\pi)^3} \frac{d^3 \mathbf{p}_{J/\psi}}{2E_{J/\psi}(2\pi)^3}. \quad (A2)$$

With one-photon-exchange approximation, one can express the squared amplitude as

$$|\mathcal{M}_{eN \to e'J/\psi N}| = \frac{4\pi\alpha}{Q^4} L^{\mu\nu} W_{\mu\nu}, \quad (A3)$$

where $L^{\mu\nu}$ is the leptonic tensor, $W_{\mu\nu}$ is the hadronic tensor, and $1/Q^4$ is the from the virtual photon propagator. Correspondingly, the phase space can be expressed as

$$dPS = \frac{d^3 \mathbf{l}'}{2E'(2\pi^3)} \widetilde{dPS}, \quad (A4)$$

where $\widetilde{dPS}$ is the phase space of $\gamma^* N \to J/\psi N$ subprocess.

To consider the virtual photon polarization, we specify a frame, in which the virtual photon momentum q and the target nucleon momentum p have only longitudinal components. For convenience, we introduce two lightlike vectors, n and $\bar{n}$, which satisfy the conditions $n^2 = \bar{n}^2 = 0$ and $n \cdot \bar{n} = 1$. Then the virtual photon momentum

$$q = (q \cdot n)\bar{n} + (q \cdot \bar{n})n. \quad (A5)$$

For transverse polarized photon,

$$d_{\mu\nu} = \sum_{\lambda=\pm} \varepsilon_\mu^*(q, \lambda)\varepsilon_\nu(q, \lambda)$$
$$= -g_{\mu\nu} + n_\mu \bar{n}_\nu + \bar{n}_\mu n_\nu, \quad (A6)$$

$$L^{\mu\nu} d_{\mu\nu} = \frac{4Q^2}{y^2(1 + \gamma^2)} \left(1 - y + \frac{1}{2}y^2 + \frac{1}{4}\gamma^2 y^2\right), \quad (A7)$$

where $y = (p \cdot q)/(p \cdot l)$, $\gamma = MQ/(p \cdot q)$, and $\varepsilon(q, \lambda)$ is the polarization vector. For longitudinal polarized photon,

$$
d_{\mu\nu} = \varepsilon_\mu^*(q, 0)\varepsilon_\nu(q, 0)
$$
$$
= \frac{1}{2}(\bar{n}_\mu n_\nu + n_\mu \bar{n}_\nu) - \frac{(q \cdot n)^2 \bar{n}_\mu \bar{n}_\nu + (q \cdot \bar{n})^2 n_\mu n_\nu}{q^2}, \tag{A8}
$$

$$
L^{\mu\nu} d_{\mu\nu} = \frac{4Q^2}{y^2(1 + \gamma^2)}\left(1 - y - \frac{1}{4}\gamma^2 y^2\right). \tag{A9}
$$

Then flux ratio between longitudinal and transverse polarized photon is

$$
\epsilon = \frac{1 - y - \frac{1}{4}\gamma^2 y^2}{1 - y + \frac{1}{2}y^2 + \frac{1}{4}\gamma^2 y^2}. \tag{A10}
$$

The cross section of the subprocess $\gamma^* N \to J/\psi N$ is

$$
d\sigma_{\gamma^* N \to J/\psi N} = \frac{|\mathcal{M}_{\gamma^* N \to J/\psi N}|^2}{4\sqrt{(q \cdot p)^2 - q^2 p^2}}\widetilde{\mathrm{dPS}}, \tag{A11}
$$

where the squared amplitude is

$$
\left|\mathcal{M}_{\gamma^* N \to J/\psi N}^{\mathrm{T}}\right|^2 = \frac{1}{2}\sum_{\lambda = \pm}\varepsilon^\mu(q, \lambda)\varepsilon^\nu(q, \lambda)W_{\mu\nu}, \tag{A12}
$$

for transverse polarized photon, and

$$
\left|\mathcal{M}_{\gamma^* N \to J/\psi N}^{\mathrm{L}}\right|^2 = \varepsilon^\mu(q, 0)\varepsilon^\nu(q, 0)W_{\mu\nu}, \tag{A13}
$$

for longitudinal polarized photon. The superscript T(L) denotes the polarization of the photon. Comparing the electroproduction and the photoproduction cross sections, one can find the relation

$$
\frac{E' d\sigma_{eN \to e'J/\psi N}}{d^3 l'} = \frac{\sqrt{(q \cdot p)^2 - q^2 p^2}}{\sqrt{(l \cdot p)^2 - l^2 p^2}}\frac{\alpha}{2(1 - \epsilon)\pi^2 Q^2}
$$
$$
\times \left(d\sigma_{\gamma^* N \to J/\psi N}^{\mathrm{T}} + \epsilon\, d\sigma_{\gamma^* N \to J/\psi N}^{\mathrm{L}}\right). \tag{A14}
$$

Since real photons only have transverse polarization states, we assume $d\sigma_{\gamma^* N \to J/\psi N}^{\mathrm{T}} = d\sigma_{\gamma N \to J/\psi N}$. Furthermore, we neglect the contribution from longitudinally polarized virtual photons for conservative estimation and obtain the relation in Eq. (6).

[1] J. J. Aubert *et al.* (E598 Collaboration), Experimental observation of a heavy particle J, Phys. Rev. Lett. **33**, 1404 (1974).

[2] J. E. Augustin *et al.* (SLAC-SP-017 Collaboration), Discovery of a narrow resonance in $e^+ e^-$ annihilation, Phys. Rev. Lett. **33**, 1406 (1974).

[3] H. X. Chen, W. Chen, X. Liu, and S. L. Zhu, The hidden-charm pentaquark and tetraquark states, Phys. Rep. **639**, 1 (2016).

[4] Y. R. Liu, H. X. Chen, W. Chen, X. Liu, and S. L. Zhu, Pentaquark and tetraquark states, Prog. Part. Nucl. Phys. **107**, 237 (2019).

[5] M. Gell-Mann, A schematic model of baryons and mesons, Phys. Lett. **8**, 214 (1964).

[6] G. Zweig, An SU(3) model for strong interaction symmetry and its breaking, Version 1, Report No. CERN-TH-401, 1964, 10.17181/CERN-TH-412.

[7] R. Aaij *et al.* (LHCb Collaboration), Observation of $J/\psi p$ resonances consistent with pentaquark states in $\Lambda_b^0 \to J/\psi K^- p$ decays, Phys. Rev. Lett. **115**, 072001 (2015).

[8] R. Aaij *et al.* (LHCb Collaboration), Observation of a narrow pentaquark state, $P_c(4312)^+$, and of two-peak structure of the $P_c(4450)^+$, Phys. Rev. Lett. **122**, 222001 (2019).

[9] A. Ali *et al.* (GlueX Collaboration), First measurement of near-threshold J/ψ exclusive photoproduction off the proton, Phys. Rev. Lett. **123**, 072001 (2019).

[10] S. Adhikari *et al.* (GlueX Collaboration), Measurement of the J/ψ photoproduction cross section over the full near-threshold kinematic region, Phys. Rev. C **108**, 025201 (2023).

[11] S. J. Brodsky, E. Chudakov, P. Hoyer, and J. M. Laget, Photoproduction of charm near threshold, Phys. Lett. B **498**, 23 (2001).

[12] Z.-E. Meziani, S. Joosten, M. Paolone, E. Chudakov, and M. Jones, A search for the LHCb charmed "pentaquark" using photoproduction of J/ψ at threshold in Hall C at Jefferson Lab, Jefferson Lab Experiment E12-16-007 (2016), https://inspirehep.net/literature/1485082.

[13] B. Duran *et al.*, Determining the gluonic gravitational form factors of the proton, Nature (London) **615**, 813 (2023).

[14] X. D. Ji, A QCD analysis of the mass structure of the nucleon, Phys. Rev. Lett. **74**, 1071 (1995).

[15] X. D. Ji, Breakup of hadron masses and energy-momentum tensor of QCD, Phys. Rev. D **52**, 271 (1995).

[16] D. Kharzeev, Quarkonium interactions in QCD, in *Proceedings of the International School of Physics "Enrico Fermi"* (IOS Press, Amsterdam, 1996), Vol. 130, pp. 105–131.

[17] D. Kharzeev, H. Satz, A. Syamtomov, and G. Zinovjev, J/ψ photoproduction and the gluon structure of the nucleon, Eur. Phys. J. C **9**, 459 (1999).

[18] A. Deur, S. J. Brodsky, and G. F. de Teramond, Connecting the hadron mass scale to the fundamental mass scale of quantum chromodynamics, Phys. Lett. B **750**, 528 (2015).

[19] M. E. Peskin, Short distance analysis for heavy quark systems: (I). Diagrammatics, Nucl. Phys. B **156**, 365 (1979).

[20] M. E. Luke, A. V. Manohar, and M. J. Savage, A QCD calculation of the interaction of quarkonium with nuclei, Phys. Lett. B **288**, 355 (1992).

[21] S. J. Brodsky and G. A. Miller, Is J/ψ-nucleon scattering dominated by the gluonic van der Waals interaction? Phys. Lett. B **412**, 125 (1997).

[22] A. B. Kaidalov and P. E. Volkovitsky, Heavy quarkonia interactions with nucleons and nuclei, Phys. Rev. Lett. **69**, 3155 (1992).

[23] T. Kawanai and S. Sasaki, Charmonium-nucleon potential from lattice QCD, Phys. Rev. D **82**, 091501(R) (2010).

[24] S. J. Brodsky, I. A. Schmidt, and G. F. de Téramond, Nuclear bound quarkonium, Phys. Rev. Lett. **64**, 1011 (1990).

[25] S. R. Beane, E. Chang, S. D. Cohen, W. Detmold, H. W. Lin, K. Orginos, A. Parreño, and M. J. Savage, Quarkonium-nucleus bound states from lattice QCD, Phys. Rev. D **91**, 114503 (2015).

[26] J. J. Wu and T. S. H. Lee, Photo-production of bound states with hidden charms, Phys. Rev. C **86**, 065203 (2012).

[27] H. Gao, T. S. H. Lee, and V. Marinov, ϕ-N bound state, Phys. Rev. C **63**, 022201(R) (2001).

[28] H. Gao, H. Huang, T. Liu, J. Ping, F. Wang, and Z. Zhao, Search for a hidden strange baryon-meson bound state from

ϕ production in a nuclear medium, Phys. Rev. C **95**, 055202 (2017).

[29] F. Huang, Z. Y. Zhang, and Y. W. Yu, $N\phi$ state in a chiral quark model, Phys. Rev. C **73**, 025207 (2006).

[30] J. He, H. Huang, D. Y. Chen, and X. Zhu, Hidden-strange molecular states and the $N\phi$ bound states via a QCD van der Waals force, Phys. Rev. D **98**, 094019 (2018).

[31] X. Qian *et al.*, Near-threshold photoproduction of phi mesons from deuterium, Phys. Lett. B **696**, 338 (2011).

[32] P. Bosted *et al.*, Search for sub-threshold photoproduction of J/Psi mesons, Phys. Rev. C **79**, 015209 (2009).

[33] Y. Hatta, M. Strikman, J. Xu, and F. Yuan, Sub-threshold J/ψ and Υ production in γA collisions, Phys. Lett. B **803**, 135321 (2020).

[34] J. J. Wu and T. S. H. Lee, Production of J/ψ on the nucleon and on deuteron targets, Phys. Rev. C **88**, 015205 (2013).

[35] S. J. Brodsky, C. R. Ji, and G. P. Lepage, Quantum chromodynamic predictions for the deuteron form-factor, Phys. Rev. Lett. **51**, 83 (1983).

[36] J. Arrington *et al.*, The Solenoidal Large Intensity Device (SoLID) for JLab 12 GeV, J. Phys. G: Nucl. Part. Phys. **50**, 110501 (2023).

[37] P. Souder, P. E. Reimer, and X. Zheng, Precision measurement of parity-violation in deep inelastic scattering over a broad kinematic range, Jefferson Lab Experiment E12-10-007 (2022), https://www.jlab.org/exp_prog/proposals/22/E12-10-007_Jeopardy.pdf.

[38] H. Gao *et al.*, Transverse spin structure of the nucleon through target single spin asymmetry in semi-inclusive deep-inelastic $(e, e'\pi^{\pm})$ reaction at Jefferson Lab, Eur. Phys. J. Plus **126**, 2 (2011).

[39] J. Arrington, N. Baltzell, A. El Alaoui, D. F. Geesaman *et al.*, Near threshold electroproduction of J/Ψ at 11 GeV, Jefferson Lab Experiment E12-12-006 (2012), https://www.jlab.org/exp_prog/proposals/12/PR12-12-006.pdf.

[40] S. Zhao, A. Camsonne, D. Marchand, M. Mazouz, N. Sparveris, S. Stepanyan, E. Voutier, and Z. W. Zhao, Double deeply virtual Compton scattering with positron beams at SoLID, Eur. Phys. J. A **57**, 240 (2021).

[41] T. S. H. Lee, S. Sakinah, and Y. Oh, Models of J/Ψ photoproduction reactions on the nucleon, Eur. Phys. J. A **58**, 252 (2022).

[42] T. S. H. Lee, Pomeron-LQCD model of J/Ψ photo-production on the nucleon, arXiv:2004.13934 [nucl-th].

[43] S. Aid *et al.* (H1 Collaboration), Elastic electroproduction of ρ^0 and J/ψ mesons at large Q^2 at HERA, Nucl. Phys. B **468**, 3 (1996); **548**, 639(E) (1999).

[44] A. Donnachie and P. V. Landshoff, Elastic scattering and diffraction dissociation, Nucl. Phys. B **244**, 322 (1984).

[45] A. Donnachie and P. V. Landshoff, Total cross-sections, Phys. Lett. B **296**, 227 (1992).

[46] A. Donnachie and P. V. Landshoff, Exclusive vector meson production at HERA, Phys. Lett. B **348**, 213 (1995).

[47] A. Donnachie and P. V. Landshoff, Small x: Two pomerons! Phys. Lett. B **437**, 408 (1998).

[48] S. Donnachie, H. G. Dosch, O. Nachtmann, and P. Landshoff, *Pomeron Physics and QCD*, Cambridge Monographs on Particle Physics, Nuclear Physics and Cosmology Series Vol. 19 (Cambridge University Press, Cambridge, 2002).

[49] J. J. Sakurai, Theory of strong interactions, Ann. Phys. **11**, 1 (1960).

[50] M. Gell-Mann and F. Zachariasen, Form-factors and vector mesons, Phys. Rev. **124**, 953 (1961).

[51] J. J. Sakurai, Vector meson dominance and high-energy electron proton inelastic scattering, Phys. Rev. Lett. **22**, 981 (1969).

[52] J. J. Sakurai and D. Schildknecht, Generalized vector dominance and inelastic electron-proton scattering, Phys. Lett. B **40**, 121 (1972).

[53] Y. S. Oh and T. S. H. Lee, One-loop corrections to omega photoproduction near threshold, Phys. Rev. C **66**, 045201 (2002).

[54] B. C. Tiburzi and G. A. Miller, Trouble in asymptopia: The Hulthen model on the light front, Phys. Rev. C **63**, 044014 (2001).

[55] M. Strikman and C. Weiss, Electron-deuteron deep-inelastic scattering with spectator nucleon tagging and final-state interactions at intermediate x, Phys. Rev. C **97**, 035209 (2018).

[56] R. B. Wiringa, V. G. J. Stoks, and R. Schiavilla, An Accurate nucleon-nucleon potential with charge independence breaking, Phys. Rev. C **51**, 38 (1995).

[57] P. A. Zyla *et al.* (Particle Data Group), Review of particle physics, Prog. Theo. Exp. Phys. **2020**, 083C01 (2020).

[58] K. Schilling and G. Wolf, How to analyze vector meson production in inelastic lepton scattering, Nucl. Phys. B **61**, 381 (1973).

[59] E. Martynov, E. Predazzi, and A. Prokudin, A universal Regge pole model for all vector meson exclusive photoproduction by real and virtual photons, Eur. Phys. J. C **26**, 271 (2002).

[60] E. Martynov, E. Predazzi, and A. Prokudin, Photoproduction of vector mesons in the soft dipole pomeron model, Phys. Rev. D **67**, 074023 (2003).

[61] R. Fiore, L. L. Jenkovszky, V. K. Magas, S. Melis, and A. Prokudin, Exclusive J/ψ electroproduction in a dual model, Phys. Rev. D **80**, 116001 (2009).

[62] M. Cai, T. Liu, and B.-Q. Ma, Bethe-Heitler lepton pair production in the deuteron breakup reaction, Chin. Phys. C **48**, 014103 (2024).